Int J Clin Exp Pathol 2019;12(1):267-274
www.ijcep.com /ISSN:1936-2625/IJCEP0086229

Original Article

Dedifferentiation patterns in DTC: is PDTC an intermediate state between DTC and ATC?

Duo Wen[1,2*], Jia-Qian Hu[1,2*], Wen-Jun Wei[1,2*], Ben Ma[1,2], Zhong-Wu Lu[1,2], Yu-Long Wang[1,2], Yu Wang[1,2], Qing-Hai Ji[1,2]

[1]*Department of Head and Neck Surgery, Fudan University Shanghai Cancer Center, Shanghai 200032, China;* [2]*Department of Oncology, Shanghai Medical College, Fudan University, Shanghai 200032, China.* [*]*Equal contributors.*

Received September 30, 2018; Accepted November 20, 2018; Epub January 1, 2019; Published January 15, 2019

Abstract: Purpose: The majority of poorly differentiated thyroid cancer (PDTC) and anaplastic thyroid cancer (ATC) are thought to dedifferentiated from differentiated thyroid cancer (DTC). PDTC is regarded as an intermediate form, through which DTC dedifferentiates into ATC. Although accumulation of gene mutations has been observed in PDTC and ATC, evidence of a direct link between DTC, PDTC, and ATC is still lacking. This work aims to illustrate if PDTC is the intermediate state between DTC and ATC. Patients and methods: Whole-exome sequencing was performed in a single patient presenting with primary papillary thyroid cancer (PTC) with simultaneous PTC, PDTC, and ATC in metastatic lymph nodes. Results: 167 nonsynonymous mutations were identified, and 24 of them were exclusive to metastatic loci. Comparison of mutational spectra revealed following results: 1) PDTC and ATC were associated with PTC-LN2 but not PTC-LN1; 2) the majority (5/6) of non-ubiquitous mutations in ATC were also present in PDTC; and 3) despite one mutation observed simultaneously in PTC-LN2, PDTC and ATC, no other associations were found between the ATC and PTC samples (primary or metastatic). Additionally, we identified five mutations (four mutations present in both PDTC and ATC, and one exclusive to ATC), including TP53 p.N107_S108delinsX, possibly related with DTC dedifferentiation. Conclusions: We observed an apparent potential, stepwise dedifferentiation process linking DTC, PDTC, and ATC, with PDTC serving as an intermediate state between DTC and ATC in one certain patient. One key mutation, combined with several low-frequency mutations, appears to underlie this dedifferentiation pathway.

Keywords: PDTC, ATC, pattern of dedifferentiation, whole-exome sequencing, intratumor heterogeneity

Introduction

Thyroid cancer is the most common malignancy of the endocrine system, with follicular cancer being the most common form [1, 2]. Follicular-derived thyroid tumors can be broadly divided into three types: differentiated thyroid cancer (DTC), poorly differentiated thyroid cancer (PDTC), and anaplastic thyroid cancer (ATC): DTC accounts for > 90% of all cancers with a relatively benign clinical presentation and good prognosis [3]. In comparison, PDTC and ATC are relatively rare, accounting for only 5-10% of all follicular-derived thyroid tumor cases, but are much more aggressive and likely to be associated with lymph node and distant metastases [4]. The median survival time of PDTC and ATC patients is 3.2 and 0.5 years, respectively; these cancers account for approximately one-third of all thyroid cancer-related deaths [5].

The mechanism of DTC dedifferentiation remains unclear. Of particular interest is the role of PDTC, which is thought to act as an intermediate form of thyroid cancer, through which DTC dedifferentiates into ATC [6]. Although poorly differentiated components are not rare in locally advanced DTC, direct pathologic evidence demonstrating a link between PDTC to ATC is lacking, with little basic research to support such a hypothesis [7]. In the largest study to date assessing gene mutations in thyroid cancer, Landa *et al*. performed exome sequencing of 341 tumor-related genes across 84 PDTC and 33 ATC samples, and found evidence that both PDTC and ATC originate from DTC cells as

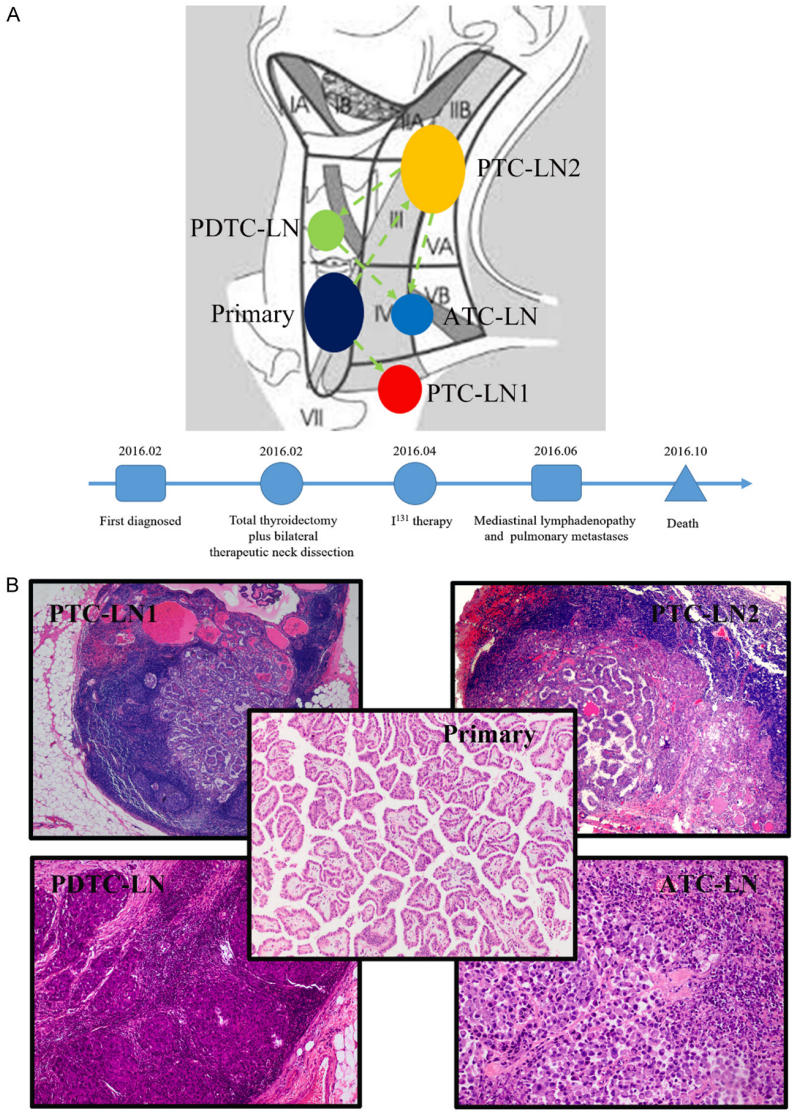

Figure 1. General information of the PTC sample. A. Schematic information of sample positions in the neck and medical history of this patient. B. Hematoxylin and eosin stain of primary tumor and lymph node metastasis.

a result of accumulating gene mutations over time, although a direct link remained elusive [8].

Here, we report a rare clinical case with well differentiated papillary thyroid cancer (PTC) diagnosed in primary tumor, but presenting with PTC, PDTC, and ATC in metastatic lymph nodes simultaneously. The biological behavior and clinical outcome of this case was more typical of ATC rather than DTC. We hypothesize that changes in the tumor microenvironment result in a stepwise, evolutional-like dedifferentiation cascade in certain tumor cells during the process of lymph node metastasis. To test this hypothesis, we examined a series of tissue samples isolated from the patient. By performing whole-exome sequencing, we evaluated the basic pattern and possible key molecules involved with the process of DTC dedifferentiation.

Material and methods

Case description

A 47-year-old female was diagnosed and treated at Fudan University Cancer Center, Shanghai, China in February 2016. Written informed consent was obtained from the patient prior to treatment. The patient first came to our clinic because of a neck mass found by routine health examination. Thyroid ultrasonography, contrast CT and fine needle aspiration (both thyroid and neck lymph node) were then performed. A diagnosis of bilateral PTC with neck lymph node metastasis was established based on preoperative examinations. No obvious signs of distant metastasis were found preoperatively. This patient was treated by total thyroidectomy plus bilateral therapeutic lymph node neck dissection.

Final pathological report confirmed bilateral PTC. On the right side, 19 lymph nodes were examined, of which 7 were positive: 5 for DTC, 1 for PDTC, and 1 for ATC. Five DTC metastatic lymph nodes were found in the left side. The primary tumors, after a thorough pathological investigation, were diagnosed as PTC solely. There were no traces of PDTC or ATC in other PTC metastatic lymph nodes, either. All of these results were reviewed by two local pathologists. The histological types of tumor were classified according to World Health Organization criteria. PDTC was defined on the basis of the Turin proposal: 1) Presence of a solid/trabecular/insular pattern of growth. 2) Absence of the conven-

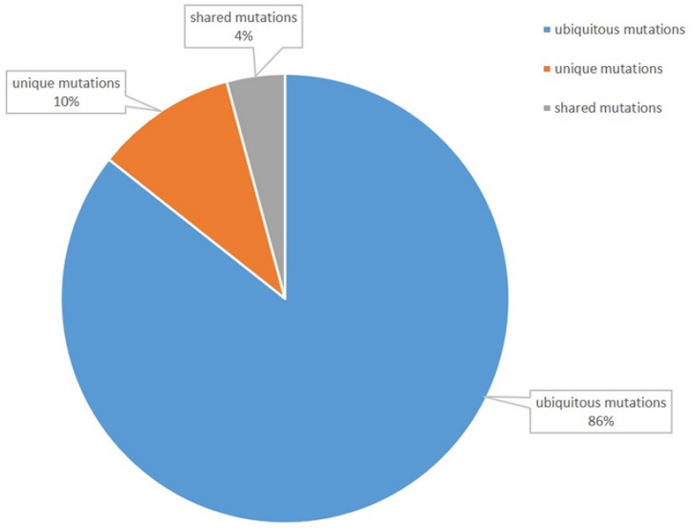

	Primary	PTC-LN1	PTC-LN2	PDTC	ATC
Ubiquitous mutations	143	143	143	143	143
Unique mutations	-	5	4	7	1
Shared mutations	-	1	3	6	5

Figure 2. Detected mutations in the PTC sample. Portions of different types of mutations illustrated in the upper figure. Exact number of different types of mutations among samples is listed in the lower table.

tional nuclear features of papillary carcinoma. 3) Presence of at least one of the following features: convoluted nuclei; mitotic activity ≥ 3 × 10 HPF, and tumor necrosis.

Two months after surgery (April 2016), radioactive iodine therapy (RAI) was started at a dose of 100 mci and whole body scan showed no signs of uptake outside the neck at that time. On follow-up examination in June 2016, mediastinal lymphadenopathy and pulmonary metastases were found. Unfortunately, due to her poor general condition, the second RAI could not be performed. This patient died in October 2016, 8 months after the operation (**Figure 1**). For the publication of this case, written informed consent was provided by the patient's husband.

DNA extraction and quality control

Samples of the primary lesion (one of the two PTC primary tumors), para-cancerous normal tissue, and ATC metastatic lesion were collected from fresh frozen tissue, and DNA was extracted using Invitrogen™ genomic DNA extraction kits (Life Technologies, USA). For two PTC and one PDTC metastatic lymph nodes, DNA was extracted from formalin-fixed and paraffin-embedded (FFPE) samples by using QIAamp® DNA FFPE Tissue kit (Qiagen, USA) and punches performed specifically in the tumor regions of the nodal metastases.

The extracted DNA was evaluated quantitatively and qualitatively according to the Q value, defined as the ratio of 129 bp and/or 305 bp amplicons to 41 bp amplicons. The Q ratio is proportional to the average target sequence coverage and is inversely proportional to the repetition rate. Q ratios > 0.4 are considered indicative of DNA extraction quality sufficient for use in whole-exome capture sequencing. A subset of mutations was selected for validation by polymerase chain reaction (PCR) amplification and Sanger sequencing.

Whole-exome sequencing and bioinformatics analysis

The NimbleGen 2.1M chip (NimbleGen Systems, Madison, WI, USA) captures exome sequences and allows for performance of DNA quality control on the Agilent 2100 Bioanalyzer (Agilent Technologies, Santa Clara, CA, USA) to ensure sufficient DNA quality for sequencing on the Genome Analyzer IIx sequencing platform (Illumina, San Diego, CA, USA).

Sequencing data quality assessment: The base mass value is expressed as the Q value, and the sequencing error rate is expressed by E; the relationship between E and the base quality can therefore be expressed as $Q = -10\log_{10}(E)$, with Q = 40 deemed acceptable. The GC content distribution was checked to evaluate the presence of A/T, G/C separation phenomenon. Sequencing data were aligned by BWA-MEM (http://bio-bwa.sourceforge.net) against the human standard genome. Sequencing reads with a ≥ 95% match to the target sequence were included in all downstream analyses.

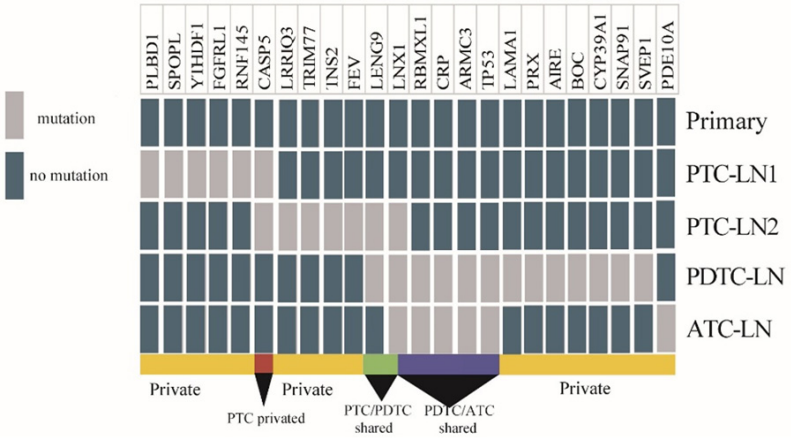

Figure 3. Map of 24 non-ubiquitous mutations. Twenty-four non-ubiquitous mutations were mapped into all of metastatic samples. Horizontal axis presents gene names that mutations were located within; Vertical axis presents different tissue samples; Grey: mutation identified; Blue: no mutation identified.

Bioinformatics analysis: Image recognition of the sequencing results were obtained, followed by removal of contaminated and linker sequences, and sequence length, number, and data yield were determined. Data were then compared against a reference genome (GRCh38/hg38) for detection of single nucleotide variations. The mutation frequency and statistical significance of identified mutation sites were validated using a combination of Exgroup (Exome Aggregation Consortium), the National Heart, Lung, and Blood Institute Exome Sequencing Project (NHLBI-ESP) exome database, (4) and Clinvar, a database for predicting the pathogenicity of gene mutations and analyzing whether mutations are likely to be pathogenic, and whether they are associated with a particular causative agent.

Results

Identification and validation of somatic mutations

For this patient, we performed exon-capture sequencing on DNA from samples of primary tumor, adjacent normal thyroid tissue, two PTC metastatic lymph nodes (PTC-LN1, PTC-LN2), one PDTC metastatic lymph node (PDTC-LN), and one ATC metastatic lymph node (ATC-LN). The average read length was 150 bp, with an average depth of 146.12, 95.07, 108.85, 146.97, 116.6, and 116.59-fold coverage, respectively. Nonsynonymous somatic point mutations and insertions and deletions (indels) that change the protein amino acid sequence were filtered and manually reviewed. Compared to normal thyroid gland tissue, a total of 167 nonsynonymous somatic point mutations and indels were identified in all samples. To facilitate the analysis, we classified the mutations and indels into three categories: 1. Ubiquitous mutations (n = 143), defined as mutations found in the primary tumor and in all of the metastatic lesions; 2. Unique mutations (n = 17), defined as mutations that were only identified in one type of metastatic sample but not in any other samples including the primary tumor; and 3. Shared mutations (n = 7), defined as mutations that were identified in at least two different metastatic samples, but were not found in the primary tumor. As shown in **Figure 2**, we mapped the regional distribution of mutations across different samples. All of 24 non-ubiquitous mutations were listed in Supplementary Table 1. From this analysis, 36 mutations were selected for validation by PCR amplification and Sanger sequencing, of which, 32 (88.9%) were specifically validated in samples in which they were initially identified.

Molecular evidence of a stepwise transformation of DTC to ATC via PDTC

To compare the mutational spectra between different metastatic lesions, we focused on those 24 non-ubiquitous mutations in this study. Data analyzing revealed four important results (**Figures 2**, **3**): 1. PTC-LN1 exhibited five unique mutations, along with one mutations also observed in PTC-LN2. In contrast, PTC-LN1 shared no mutations with the PDTC or ATC samples. 2. In addition to the one mutation shared with PTC-LN1, PTC-LN2 harbored four unique mutations, along with one mutation shared with PDTC, and other one mutation simultaneously shared with PDTC and ATC. 3. The PDTC sample exhibited seven unique mutations, four PDTC/ATC shared mutations and one PTC-LN2/PDTC/ATC shared mutation. 4. The ATC sample contained one unique mutations and five sh-

Table 1. Potential PTC dedifferentiation-related mutations

Gene	Chr[d]	Pos[e]	Ref[f]	Alt[g]	ExonicFunc	AA change[h]	Primary[a]		PDTC-LN[b]		ATC-LN[c]	
							AP[i]	Cov[j]	AP	Cov	AP	Cov
RBMXL1	chr1	89449509	T	-	Frameshift deletion	p.G71A	0	121	0.11	55	0.28	67
CRP	chr1	159683661	G	A	Nonsynonymous	p.A110V	0	110	0.31	134	0.18	178
ARMC3	chr10	23326291	GA	-	Frameshift deletion	p.R834fs p.R571fs p.R827fs	0	41	0.21	42	0.18	45
TP53	chr17	7577566	-	A	Stopgain	-	0	68	0.44	52	0.34	50
PDE10A	chr6	166075488	G	T	Nonsynonymous	p.P5H	0	15	0	11	0.33	12

a. Primary: primary tumor; b. PDTC-LN: lymph node with poorly differentiated cancer metastases; c. ATC-LN: lymph node with anaplastic thyroid carcinoma metastases; d. Chr: chromosome; e. Pos: position; f. Ref: reference Genomic sequences; g. Alt: Alternative genomic bases; h. AA change, Amino acid changes; i. AP: Alternative allelic portion; j. Cov, coverages.

Table 2. Reported second generation sequencing results of PDTC/ATC

	Landa, 2016	Sykorova, 2015	Kunstman, 2015	Jeon, 2016
Sample size				
PDTC	84	3	0	0
ATC	33	5	22	11
Sources	FFPE+FFT	FFT	FFPE	FFPE
Methods	Targeted gene exon sequencing	Targeted gene exon sequencing	Whole exome sequencing	Targeted gene exon sequencing
	N = 341	N = 94		N = 505
Other methods	Gene expression microarrays	-	-	Protein spectrometry

ared mutations as mentioned above. All of these five shared mutations were also seen in the PDTC sample.

Identification of PTC dedifferentiation-related mutations

In our sequencing data, we found a total of four mutations shared between PDTC and ATC, along with one mutation unique to ATC (**Table 1**). Among these mutations, the role of the tumor suppressor gene TP53 is well-established, with newer estimates suggesting a mutation frequency up to 50% higher than that of earlier reports [9, 10]. The p.N107_S108delinsX mutation of TP53 identified in this study is a stopgain mutation, in which deletion of the stop codon results in a decrease in the efficiency of transcriptional translation. We also identified mutations in PDE10A, a gene that has been linked to tumorigenesis in non-small cell lung cancer [11].

All of mutations identified in this study were further compared against the two thyroid databases of the The Cancer Genome Atlas (TCGA). With the exception of TP53, all of the mutations identified in this study were low-frequency mutations. Examples include ARMC3 and CRP, for which mutations were observed in only one PTC sample. No mutations were detected in either PDE10A or RBMXL1.

Discussion

Dedifferentiation of DTC is an important factor in PTC diagnosis, having a significant impact on both therapeutic intervention strategy and clinical outcome [12]. Tumor dedifferentiation, as is widely acknowledged, can result in advanced invasion and metastasis, limiting surgical options for certain patients. RAI is another therapy in the treatment of DTC apart from surgery, whose success depends on the presence of sodium-iodide symporters (NIS) on the surface of thyroid follicular cells [13]. Decreased NIS activity caused by tumor dedifferentiation is likely to result in a diminished response to RAI, reducing the possible chance of a successful outcome [14]. Dedifferentiation is a major cause of RAI failure [4, 15]. For those who are diagnosed with RAI refractory DTC, we now have targeted drugs indicated for their situation. Unfortunately, there are currently no targeted drugs approved for use against either ATC or PDTC [16, 17]. Better methods for identifying tumor dedifferentiation in early stage patients, in combination with targeted thera-

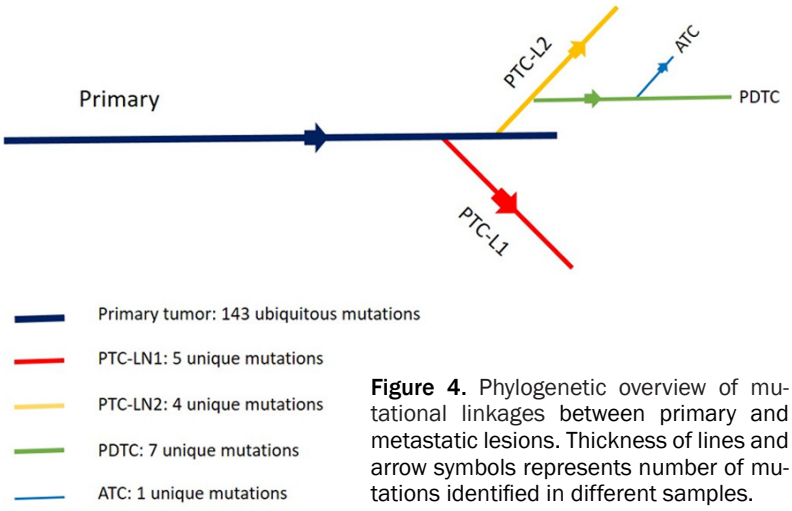

Figure 4. Phylogenetic overview of mutational linkages between primary and metastatic lesions. Thickness of lines and arrow symbols represents number of mutations identified in different samples.

pies effectively against dedifferentiated DTC, represent important unmet goals in thyroid cancer research.

A better understanding of dedifferentiation is the first step to treat these patients. To date, two basic models have been proposed to this end: stepwise transformation from DTC to ATC via PDTC, and the de novo model of independent transformation from DTC to ATC and PDTC. [18] Unfortunately, both models lack sufficient evidence, yielding further research in this field [19]. Our hospital has treated 60 patients with PDTC or ATC between 2006 and 2015, including 5 cases of ATC in a DTC background and 18 cases of DTC and PDTC in the same tumor. However, no clear coexistence of DTC, PDTC, and ATC within a single primary lesion has been observed, so we cannot confirm direct transformation from PDTC to ATC.

With recent advances in next-generation sequencing, significant advances have been made in terms of quantitative data analysis. Xu *et* al. assessed the role of known mutations in PTC. A total of 87 PDTC and 71 ATC cases, drawn from four publications (**Table 2**): the analysis showed that both PDTC and ATC are the results of DTC cells gradually accumulating mutations over time [20-22]. Delving deeper into these data, ATC lesions exhibited higher mutational frequencies in TERT, as well as in the PIK3CA-PTEN pathway, tumor suppressors, and DNA repair genes [23, 24]. However, none of these studies provided direct supporting evidence of transformation of DTC to ATC via PDTC. Furthermore, most of the studies used targeted gene exome sequencing, which cannot evaluate the whole genome.

In this study, we proposed a model for exploring the patterns of, and mechanisms underlying, DTC dedifferentiation in a single patient who had well-differentiated papillary thyroid cancer (PTC) diagnosed in a primary tumor, but with PTC, PDTC, and ATC in metastatic lymph nodes simultaneously. To that end, we employed whole-exome capture sequencing to detect and compare the mutational spectra among the different samples. Results showed three important findings. First, the majority (5/6; 77.8%) of the non-ubiquitous mutations in the ATC sample were also present in the PDTC sample. Second, with the exception of one PTC-LN2/PDTC/ATC shared mutation, there was no other common mutation existing between ATC and PTC samples (primary or metastatic). Finally, the PTC-LN2/PDTC/ATC shared mutation represent the only mutational link between the PTC and dedifferentiated samples, meaning that PTC-LN1 was unrelated to the PDTC and ATC lesions. On observation of the close relationship between PDTC and ATC, we speculated that the dedifferentiation from PDTC to ATC occurred more likely during the metastatic phase of the disease, rather than progression from different primary tumor subclones separately. It suggests a relatively straightforward stepwise transformation of DTC to ATC via PDTC, which acts as an essential intermediate state. A phylogenetic overview of this mutational linkage is shown in **Figure 4**.

Mutations shared between PDTC and ATC are the most likely drivers of the PTC dedifferentiation process, while unique ATC mutations may also play a role in this transformation. Our study identified the p.N107_S108delinsX mutation of TP53. This mutation may act as a switch in PTC dedifferentiation. Mutations in the PDE10A gene were also revealed by sequencing. Notably, this gene has been reported to be related with tumorigenesis in non-small cell lung cancer [11]. Other mutations identified in this study have not been linked to tumorigenesis, and

their role in PTC dedifferentiation and tumor progression are unclear. More studies need to be done to discover their biological functions.

However, it is the most likely explanation but not the only one. Actually, we could not rule out the possibility that PDTC and ATC metastatic lesions were arise from the same subclone in the primary tumor and developed in different lymph node with a parallel way. The reason, that those unique and shared mutations identified in PDTC and ATC samples have not been detected in the primary tumor, may be caused by tumor purity and heterogeneity. This possibility is relatively low, because the locations of PDTC and ATC lymph nodes are the furthest from the primary tumor than other PTC metastatic lesions. To exclude this possibility to the maximum extent, multipoint sampling and microdissection methods are necessary during sample collection.

Since lymphatic reflux represents a self-sustained dynamic system, there may be internal cross-connection; theoretically, the primary cells of the ATC metastases could have originated from upstream PDTC metastases, or from PTC metastases. However, based upon our sequencing results, the non-ubiquitous mutations carried by the ATC metastases did not intersect with PTC-LN1. Meanwhile, two mutations identified in the PDTC metastases were shared with PTC-LN2, suggesting that PDTC is likely to be a necessary intermediate state between DTC and ATC. To further limit the influence of the complex lymph node cross-connection, a full exome sequencing of all confirmed positive lymph nodes is indispensable.

The last and most important limitation of this study is its single-case design. This case may not be reflective enough of the wider population, for the mutations identified could be case-sensitive, which means these genes may only mutate in this case. Accordingly, the possibility of other dedifferentiation patterns in DTC cannot be ruled out. Therefore, to address this limitation, more cases need to be collected and more aspects, such as RAI therapy and targeted drug clinical trials, should also be taken into account in the future.

In conclusion, our data provide evidence of a possible link between the mutational profile of lesions and their dedifferentiation status. In this model, the transformation process from PTC to ATC was more likely stepwise. PDTC may play an important role as an intermediary between DTC and ATC, with the transformation driven by a single key mutation in combination with several low-frequency mutations.

Acknowledgements

The abstract of this paper was presented at the 87th annual meeting of the American Thyroid Association (ATA) as a poster presentation. The poster's abstract was published in Thyroid. Volume: 27 Issue S1: October 1, 2017. http://doi.org/10.1089/thy.2017.29050.sc.abstracts. This work was supported by funds from the National Natural Science Foundation of China, 81572622 to Qing-Hai Ji; 81502317 to Wei-Wen Jun, 81472498 and 81772851 to Yu-Long Wang.

Disclosure of conflict of interest

None.

Address correspondence to: Qing-Hai Ji and Yu Wang, Department of Head and Neck Surgery, Fudan University Shanghai Cancer Center, Shanghai 200032, China; Department of Oncology, Shanghai Medical College, Fudan University, Shanghai 200032, China. Tel: 0086-021-64175590; Fax: 0086-021-64175590; E-mail: jq_hai@126.com (QHJ); wangyu@shca.org.cn (YW)

References

[1] Sherma SI. Thyroid carcinoma. Lancet 2003; 361: 501-511.

[2] Schlumberger MJ. Papillary and follicular thyroid carcinoma. N Engl J Med 1998; 338: 297-306.

[3] Pacini F, Castagna M, Brilli L, Pentheroudakis G; ESMO Guidelines Working Group. Thyroid cancer: ESMO clinical practice guidelines for diagnosis, treatment and follow-up. Ann Oncol 2012; 23 Suppl 7: vii110-9.

[4] Viola D, Valerio L, Molinaro E, Agate L, Bottici V, Biagini A, Lorusso L, Cappagli V, Pieruzzi L and Giani C. Treatment of advanced thyroid cancer with targeted therapies: ten years of experience. Endocr Relat Cancer 2016; 23: R185-R205.

[5] Molinaro E, Romei C, Biagini A, Sabini E, Agate L, Mazzeo S, Materazzi G, Sellari-Franceschini S, Ribechini A and Torregrossa L. Anaplastic thyroid carcinoma: from clinicopathology to ge-

netics and advanced therapies. Nat Rev Endocrinol 2017; 13: 644-660.
[6] Lee DY, Won JK, Lee SH, Park DJ, Jung KC, Sung MW, Wu HG, Kim KH, Park YJ and Hah JH. Changes of clinicopathologic characteristics and survival outcomes of anaplastic and poorly differentiated thyroid carcinoma. Thyroid 2016; 26: 404-413.
[7] Sasanakietkul T, Murtha TD, Javid M, Korah R and Carling T. Epigenetic modifications in poorly differentiated and anaplastic thyroid cancer. Mol Cell Endocrinol 2018; 469: 23-37.
[8] Landa I, Ibrahimpasic T, Boucai L, Sinha R, Knauf JA, Shah RH, Dogan S, Ricarte-Filho JC, Krishnamoorthy GP and Xu B. Genomic and transcriptomic hallmarks of poorly differentiated and anaplastic thyroid cancers. J Clin Invest 2016; 126: 1052-66.
[9] Stengel A, Kern W, Haferlach T, Meggendorfer M, Fasan A and Haferlach C. The impact of TP53 mutations and TP53 deletions on survival varies between AML, ALL, MDS and CLL: an analysis of 3307 cases. Leukemia 2017; 31: 705-711.
[10] Forbes SA, Beare D, Bindal N, Bamford S, Ward S, Cole C, Jia M, Kok C, Boutselakis H and De T. COSMIC: high-resolution cancer genetics using the catalogue of somatic mutations in cancer. Curr Protoc Hum Genet 2016; 91: 10.11.1-10.11.37.
[11] Zhu B, Lindsey A, Li N, Lee K, Ramirez-Alcantara V, Canzoneri JC, Fajardo A, da Silva LM, Thomas M and Piazza JT. Phosphodiesterase 10A is overexpressed in lung tumor cells and inhibitors selectively suppress growth by blocking β-catenin and MAPK signaling. Oncotarget 2017; 8: 69264-69280.
[12] Haugen BR, Alexander EK, Bible KC, Doherty GM, Mandel SJ, Nikiforov YE, Pacini F, Randolph GW, Sawka AM and Schlumberger M. 2015 American Thyroid Association management guidelines for adult patients with thyroid nodules and differentiated thyroid cancer: the American Thyroid Association guidelines task force on thyroid nodules and differentiated thyroid cancer. Thyroid 2016; 26: 1-133.
[13] Seregni E, Mallia A, Chiesa C, Scaramellini G, Massimino M and Bombardieri E. Radioiodine therapy of differentiated thyroid cancer. In: editors. Nuclear medicine therapy. Springer; 2013. pp. 133-153.
[14] Lakshmanan A, Scarberry D, Shen DH and Jhiang SM. Modulation of sodium iodide symporter in thyroid cancer. Horm Cancer 2014; 5: 363-373.
[15] Fröhlich E and Wahl R. The current role of targeted therapies to induce radioiodine uptake in thyroid cancer. Cancer Treat Rev 2014; 40: 665-674.
[16] Gilliland FD, Hunt WC, Morris DM and Key CR. Prognostic factors for thyroid carcinoma. A population-based study of 15,698 cases from the Surveillance, Epidemiology and End Results (SEER) program 1973-1991. Cancer 1997; 79: 564-573.
[17] Mazzaferri EL and Kloos RT. Clinical review 128: current approaches to primary therapy for papillary and follicular thyroid cancer. J Clin Endocrinol Metab 2001; 86: 1447-1463.
[18] Dellaire G, Berman JN and Arceci RJ. Cancer genomics: from bench to personalized medicine. Academic Press; 2013.
[19] Xing M. Molecular pathogenesis and mechanisms of thyroid cancer. Nat Rev Cancer 2013; 13: 184-199.
[20] Sykorova V, Dvorakova S, Vcelak J, Vaclavikova E, Halkova T, Kodetova D, Lastuvka P, Betka J, Vlcek P and Reboun M. Search for new genetic biomarkers in poorly differentiated and anaplastic thyroid carcinomas using next generation sequencing. Anticancer Res 2015; 35: 2029-2036.
[21] Kunstman JW, Juhlin CC, Goh G, Brown TC, Stenman A, Healy JM, Rubinstein JC, Choi M, Kiss N and Nelson-Williams C. Characterization of the mutational landscape of anaplastic thyroid cancer via whole-exome sequencing. Hum Mol Genet 2015; 24: 2318-2329.
[22] Jeon MJ, Chun SM, Kim D, Kwon H, Jang EK, Kim TY, Kim WB, Shong YK, Jang SJ and Song DE. Genomic alterations of anaplastic thyroid carcinoma detected by targeted massive parallel sequencing in a BRAFV600E mutation-prevalent area. Thyroid 2016; 26: 683-690.
[23] Xu B and Ghossein R. Genomic landscape of poorly differentiated and anaplastic thyroid carcinoma. Endocr Pathol 2016; 27: 205-212.
[24] Rosove MH, Peddi PF and Glaspy JA. BRAF V600E inhibition in anaplastic thyroid cancer. N Engl J Med 2013; 368: 684-685.

Supplementary Table 1. Unique and shared mutations in all of lymph node metastasis specimens

Gene	Chr	Pos	Ref	Alt	Alternation type	AA Change	PRIMARY		PTC-LN1		PTC-LN2		PDTC		ATC	
							AP	Cov	AP	Cov	AP	Cov	AP	Cov	AP	Cov
Unique mutations of PTC-LN1																
PLBD1	chr12	14720590	T	G	Nonsynonymous SNV	p.Q14P	0	19	0.22	9	0	28	0	20	0	20
SPOPL	chr2	139326516	G	A	Nonsynonymous SNV	p.D349N	0	65	0.21	47	0	47	0	34	0	35
YTHDF1	chr20	61834858	G	T	Nonsynonymous SNV	p.S145Y	0	44	0.23	35	0	53	0	25	0	45
FGFRL1	chr4	1019055	CA	-	Frameshift deletion	p.H479fs	0	66	0.23	40	0	100	0	54	0	54
RNF145	chr5	158630629	-	TT	Frameshift insertion	p.N29fs; p.N16fs; p.N13fs;	0	115	0.17	47	0	91	0	152	0	62
Mutations shared by PTC-LN1 and PTC-LN2																
CASP5	chr11	104878040	-	T	Frameshift insertion	p.T10fs; p.T81fs; p.T68fs	0	86	0.16	64	0.14	65	0	73	0	70
Unique mutations of PTC-LN2																
LRRIQ3	chr1	74575212	-	T	Frameshift insertion	p.Q245fs	0	183	0	101	0.13	191	0	117	0	115
TRIM77	chr11	89444610	-	A	Frameshift insertion	p.W148fs	0	165	0	81	0.15	151	0	104	0	141
TNS2	chr12	53451822	G	A	Nonsynonymous SNV	p.G354D; p.G344D; p.G220D	0	6	0	5	0.29	7	0	7	0	8
FEV	chr2	219846580	A	G	Nonsynonymous SNV	p.S176P	0	6	0	6	0.29	14	0	7	0	8
Mutations shared by PTC-LN2 and PDTC																
LENG9	chr19	54974774	A	T	Nonsynonymous SNV	p.M1K	0	7	0	4	0.62	8	0.73	11	0	5
Mutations shared by PDTC-LN2, PDTC and ATC																
LNX1	chr4	54327211	-	A	Splice	-	0	49	0	35	0.16	31	0.19	31	0.22	27
Mutations shared by PDTC and ATC																
RBMXL1	chr1	89449509	T	-	Frameshift deletion	p.G71A	0	121	0	54	0	82	0.11	55	0.28	67
CRP	chr1	159683661	G	A	Nonsynonymous SNV	p.A110V	0	110	0	94	0	97	0.31	134	0.18	178
ARMC3	chr10	23326291	GA	-	Frameshift deletion	p.R571fs; p.R827fs; p.R834fs	0	41	0	42	0	44	0.21	42	0.0.9	45
TP53	chr17	7577566	-	A	Stopgain	-	0	68	0	56	0	59	0.44	52	0.34	50
Unique mutations of PDTC																
LAMA1	chr18	7117665	G	A	Stopgain	p.Q19X	0	44	0	7	0	36	0.33	24	0	30
PRX	chr19	40901323	C	T	Nonsynonymous SNV	p.G979E	0	46	0	22	0	50	0.28	18	0	31
AIRE	chr21	45712283	C	T	Nonsynonymous SNV	p.P365L	0	20	0	9	0	19	0.67	6	0	13
BOC	chr3	112998209	T	A	Nonsynonymous SNV	p.Y644N; p.Y643N	0	38	0	42	0	67	0.25	28	0	38
CYP39A1	chr6	46620316	C	-	Frameshift deletion	p.E2fs	0	76	0	49	0	65	0.23	30	0	67
SNAP91	chr6	84269884	A	C	Nonsynonymous SNV	p.V550G; p.V827G; p.V733G; p.V857G; p.V766G	0	55	0	30	0	67	0.19	48	0	43
SVEP1	chr9	113173407	G	A	Nonsynonymous SNV	p.P2195L	0	41	0	55	0	39	0.33	46	0	60
Unique mutations of ATC																
PDE10A	chr6	166075488	G	T	Nonsynonymous SNV	p.P5H	0	15	0	9	0	4	0	11	0.33	12

Primary: primary tumor; PDTC-LN: lymph node with poorly differentiated cancer metastases; ATC-LN: lymph node with anaplastic thyroid carcinoma metastases; Chr: chromosome; Pos: position; Ref: reference Genomic sequences; Alt: Alternative genomic bases; AA change, Amino acid changes; AP: Alternative allelic portion; Cov, coverages.